Hui Zhang, Luca Nizzetto, Xinbin Feng, Katrine Borgå, Jonas Sommar, Xuewu Fu, Hua Zhang, Gan Zhang, and Thorjørn Larssen. Environmental Science & Technology 2019 53(9), 4869-4879.

Assessing the air-surface exchange and fate of mercury in a subtropical forest using a novel passive exchange-meter device

Hui Zhang[†], Luca Nizzetto[*⁄⁄#], Xinbin Feng[*†‡§], Katrine Borga[⁄⁄⊥], Jonas Sommar[†], Xuewu Fu[*†‡], Hua Zhang[†], Gan Zhang[∇], Thorjørn Larssen[⁄⁄]

[†]State Key Laboratory of Environmental Geochemistry, Institute of Geochemistry, Chinese Academy of Sciences, 99 Lincheng West Road, Guiyang, 550081, China

[‡] CAS Center for Excellence in Quaternary Science and Global Change，Xi'an, 710061, China

[§] University of Chinese Academy of Sciences, Beijing 100049, China

[⁄⁄]Norwegian Institute for Water Research, Oslo, Norway

[⊥]Department of Biosciences, University of Oslo, Oslo, Norway

[#] Research Centre for Toxic Compounds in the Environment, Masaryk University, Brno, Czech Republic

[∇] State Key Laboratory of Organic Geochemistry, Guangzhou Institute of Geochemistry, Chinese Academy of Sciences, Guangzhou, China

*Corresponding author: Xinbin Feng, Xuewu Fu and Luca luca.nizzetto

Abstract: A novel passive exchange meter (EM) device was developed to assess air-surface exchange and leaching of Hg in a forest floor. Flux measurements were carried out in a subtropical forest ecosystem during a full year. Over 40% of the Hg fixed in fresh forest litter was remobilized in less than 60 days in warm and humid conditions as a response to rapid turnover of labile organic matter (OM). A two-blocks experiment including understory and clearing showed that losses of Hg co-varied with seasonal conditions , and was significantly affected by forest coverage. The process controlling the bulk loss of total Hg from the litter was volatilization, which typically represented 76% to 96% of the loss processes *(F_{loss})*. F_{loss} ranged 520-1370 ng m^{-2} d^{-1} and 165-942 ng m^{-2} d^{-1}, in the understory and clearing, respectively. On a yearly basis, deposition of airborne Hg exceeded the total losses by a factor 2.5 in the clearing and 1.5 in the understory. Vegetation litter in this subtropical forest therefore represented a net sink of atmospheric Hg. This study provided a nvel approach to Hg air-soil exchange measurements and further insights on the link between Hg remobilization and OM turnover along with its environmental drivers.

TOC art:

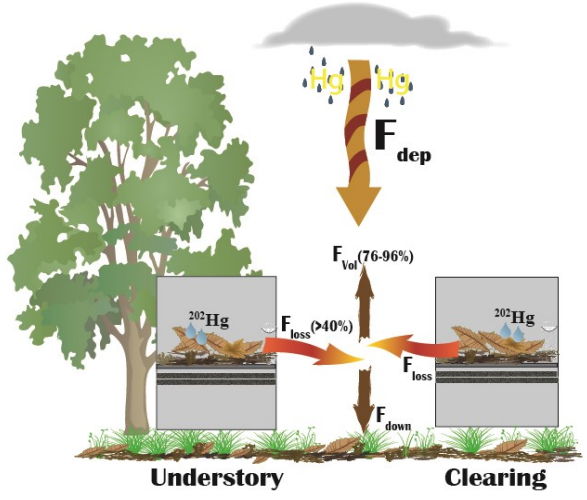
Hg
Hg
F dep
F Vol (76-96%)
202Hg
F loss (>40%)
202Hg
F loss
F down
Understory
Clearing

Introduction

Hg is an ubiquitous neurotoxic pollutant. Anthropogenic emissions of Hg to the atmosphere are primarily in the form of elemental mercury (Hg(0)) and divalent mercury (Hg(II)), while redox chemistry controls the transition between these two species. Hg(0) is relatively volatile, whereas Hg(II) is less volatile, more soluble and rapidly scavenged by wet depositions and direct adsorption to soils and vegetation[1-4]. Evidences suggest that scavenging by forests is an important sink of atmospheric Hg while organic soils and vegetation represent important long-term reservoirs[5-8]. Once in the soil Hg can undergo a methylation reaction to form a highly neurotoxic and bioaccumulative species.

Earlier assessments estimated that the global annual Hg deposition through litterfall is 1180 ± 710 Mg yr^{-1}, while the OM bounded Hg in background soils and vegetation is in the order of 240,000 Mg, globally [7, 9]. This figure exceeds of two orders of magnitude the steady state atmospheric budget of total Hg (~5,000 Mg) suggesting that re-mobilization from aging organic matter can easily affect atmospheric loads and, consequently, global distribution. Hg emitted from soil organic matter (OM) and biomasses is calculated to represent 31% of the sum of total anthropogenic secondary emissions and natural sources[4].

Hg(II) and Hg(0) can be adsorbed to OM through ionic exchange and simple condensation processes on organic surfaces, respectively[10-12]. These bounds are reversible and Hg can be re-emitted if environmental conditions of OM characteristics change over time[10, 13]. The predominant pool of Hg associated to OM is thought to be taken-up by the foliage and covalently fixed . To this regard, reduced sulphur groups in the OM efficiently bind Hg (II), preventing reduction processes[9, 14, 15]. Recent studies showed that most Hg in plant leaves is sequestered as divalent mercury-sulphur nanoparticles[11]. This promotes long term storage in vegetation and soil. The re-emission of Hg to the atmosphere is therefore expectedly subordinated to the degradation of these binding structures. In nature this can occur accidentally through fires, or naturally and more diffusely through biochemical degradations.

Despite the potentially high relevance of the re-mobilization from vegetated soils for the global Hg mass balance, the coupling between volatilization and the turnover of labile organic matter is poorly understood. Empirical assessments are available only from few controlled laboratory experiments[16-18] which showed a correlation between Hg volatilization and OM degradation. In field assessments, correlative studies have shown a potential link between these two processes[18, 19], but a causal relationship could not be confirmed. Covariance of OM turnover with temperature and humidity can in fact blur causal relationships.

Laboratory experiments demonstrated slow mobilization of only a relatively minor fraction (between 5 and 23%) of the mass of Hg initially bound to OM, in response to a two-fold loss in the OM mass during a 18 months-long observations[18]. The use of traditional deposimeters to assess air-OM exchange does however not allow disentangling the influence of co-occuring processes affecting Hg and OM mass budgets. Continuous depositions of "fresh" airborne Hg during OM ageing may in fact mask volatilization fluxes[20].

In order to study Hg mobilization from OM in forest floors at the net of atmospheric depositionsin in-situ OM ageing experiments, we developed a novel passive exchange meter (EM) that, utilizing a mass balance approach, simultaneously and dynamically resolves OM and Hg budgets in vegetation litter over arbitrarily chosen integrated time periods. To assess causality in the relationship between litter dry mass and Hg re-mobilization and assess the entity of Hg fluxes under fast OM turnover, an experiment was conducted in a subtropical humid forest of southern China, subjected to monsoon climate. The subtropical monsoon climatic conditions maximize the seasonal variance of OM degradation assessed here through losses of litter dry weight and losses in organic carbon content from forest litter.

To control for possible spurious correlations between Hg re-mobilization and OM degradation (possibly mediated by precipitation, air humidity or temperature as lurking variables), the experiment was conducted in two blocks using 5 replicated EMs deployed in a forest plot under a dense canopy (estimated leaf area index was 5), and 5 replicated EM in an adjacent (less than 30 m distant) understory gap (clearing diameter was about 10 m). Previous studies showed that canopy gaps significantly inhibit degradation of litter, while experiencing nearly identical conditions of air temperature, humidity and precipitations[21].

Material and methods

Site description

The study site is located in the Dinghu National Nature Reserve (DNNR) area in mid-western Guangdong province, China (Figure 1). DNNR is part of the "Man and the Biosphere" **(**MAB**)** Programme of United Nations Educational, Scientific and Cultural Organization **(**UNESCO) network of protected areas. It has typical subtropical monsoon climate with hot and wet seasons (from Apr. to Sep.) and dry and cold seasons (from Oct. to Mar.) The annual average temperature is 20.9 °C with the hottest month in July (average 26.0 °C) and the coldest in January (average 12.6 °C). The annual average rainfall is 1929 mm,[22] with 75% of precipitations occurring from March to August[23]. The land use is characterized by evergreen coniferous and broad-leaved mixed forests. Dominant tree species are broad-leaves (mainly *Schima superba and Castanopsis chinensis*) and pine needles (mainly *Pinus massoniana*). Surface litter covers 80%-90% of the ground with a thickness of 1-3 cm[24].

Exchange Meters

The EM (Figure 2 and Figure S1) consists of a stainless-steel tripod with a cylindrical cross-section holding an open borosilicate glass cylinder (diameter 16 cm, height 25 cm). The glass cylinder seals up two pieces of silver mesh discs (pore size of 0.8 µm, thickness 51 µm, SPI-Pore™) placed at its base. Above the silver mesh, a nickel net (<2 mm mesh) is placed, holding a sample of litter collected in-situ and spiked with a known amount of ^{202}Hg(II). ^{202}Hg(II) is used as a field reference to determine the volatilization and leaching fluxes (as described in a following section). This isotope is an ideal surrogate for tracking fate processes in OM as the bulk of mercury bound to forest litter is in the form of Hg(II). This is supported by previous findings showing that mercury in foliage is prevalently oxidized and exists in complex forms such as organic Hg-S species[6, 11, 25-27]. A small portion of Hg(II) in litterfall may convert into Hg(0) from time to time through Hg(II) reduction, but in this form will rapidly be released back to the atmosphere[28, 29].

EM handling and sampling

For each sampling period forest litter (including broad-leaves (mainly *Schima superba and Castanopsis chinensis*) and pine needles (mainly *Pinus massoniana*)) was collected from the forest site. In order to determine the water content an aliquote of the litter was vacuum dried for 24 h . Large dead leaves

and detritus present in the remaining litter was mechanically broke-down to achieve a texture with the largest pieces in the order of 1 cm^2. This was done to allow adequate homogeneization and distribution of samples in repicaltes EMs. The remaining litter was then spiked with 2.00 µg of inorganic divalent ^{202}Hg by adding 100 mL of 20ng/ml $^{202}Hg(NO_3)_2$ solution to 200 g (dw) of litter. The solution of $^{202}Hg^{2+}$ was prepared by dissolving 1 mg of ^{202}HgO in 1 ml of HNO_3 solution and diluted to 20 ng ml^{-1} by adding Milli-Q water. The spiked litter was transferred into an ambered borosilicate glass jar, vigorously shaken by hand for several minutes and stored in the dark jar for at least 24 h before deployment in the field. This procedure was carried out to allow homogenization and partial re-distribution and of ^{202}Hg in the litter sample. The spiked litter was then distributed in situ into 10 aliquots of 20 g each and deployed in different EMs (five in understory and five in the adjacent clearing) (Figure S1). The EMs were deployed so that the spiked litter sample was only a few cm above the soil level to approximate natural exposure conditions. After field deployment, the spiked litter was sampled twice: 6 h after deployment and after two months to calculate changes in the masses of Hg (THg), ^{202}Hg, dry organic matter, organic carbon (OC), N and water content before (t_0) and after (t_f) the exposure period. Sampling at t_0 was conducted by collecting 5 g of litter from each EM. These were carefully sealed, individually, into plastic bags and brought back to the laboratory. At t_f the remaining litter was collected and handled in a similar way. At t_f silver mashes, conceived to sample the leaching flux of $^{202}Hg(II)$ were also retrieved and stored in sealed bags. Before analysis, litter and silver meshes were stored at 4 ºC. This procedure was repeated 6 times covering time intervals of two months throughout a full year.

Hg analysis

Litter samples were freeze dried and grinded to a fine powder in a pre-cleaned food blender (200 meshes). The blender was extensively cleaned with Milli-Q water and ethanol between different sample batches to prevent cross contamination[20, 30]. THg in litter samples were determined by Zeeman Lumex mercury analyzer (model RA915+, Lumex Co. Inc., Russia) attached with Pyro-91 thermal decomposition accessory from Lumex Ltd. The solid samples were directly decomposed in atomizer chamber at 800 °C with the aided catalytic action. THg was then measured by RA-915t analyzer[31]. Standard reference samples were measured every 10 field samples yielding recoveries in the range of 95%–105%. GBW10020 (GSB-11) was used as the litter Hg standard. Approximately 0.15 g of the samples were digested in 50 mL of freshly mixed HNO_3/H_2SO_4 (4:1 v/v) for 6 h at 95 °C in a water bath[32, 33]. The digested solution was then diluted by adding Mili-Q water to a volume of 25 mL. For Hg isotope analysis, the analyte preconcentrated by BrCl oxidation, $SnCl_2$ reduction, purge and trap step onto a gold trap was thermo-desorbed quadrupole inductively coupled plasma mass spectrometry (ICP–MS; Agilent 7700X). The detection limit was 100 pg/L for Hg[34-37].

For the analysis of ^{202}Hg in the silver meshes, filters were transferred in quartz glass tubes into a furnace. The quartz tube was subsequently connected to a generator of Hg-free air (Nitrogen gas, ≤ 0.1 ng m^{-3}). Temperature was increased to ~450 °C. The silver amalgam was then decomposed into Hg(0) vapor, which was brought by the air stream into a bubbler containing an acidic $KMnO_4$ solution that quantitatively oxidized the generated Hg(0). An aliquot of the $KMnO_4$ solution was used for analysis. Prior to analysis, excess $KMnO_4$ was reduced with $NH_2OH•HCl$ (aq) and subsequently Hg(II) (aq) was back-reduced to Hg(0) by addition of $SnCl_2$ (aq). Hg(0) was subsequentely purged from the solution and pre-concentrated onto a gold trap to be finally quantified by ICP-MS.

QA/QC

All borosilicate glass cylinders were pre-cleaned following the US EPA Method 1631 (https://nepis.epa.gov/Exe/ZyPURL.cgi?Dockey=P1008IW8.txt). Briefly, the outside and inside surfaces of the Ems glass cylinders were first washed with laboratory analytic grade acetone in a fume hood, then washed with alkaline detergent, and finally rinsed five times with de-ionised water. The cylinders were immersed in 3.5 % HNO_3 for 6 hours at 65-75 ºC through submerging the cylinders in a polyethylene bucket containing a HNO_3 solution. We ensured all the cylinder surfaces were in contact with the HNO_3 solution. After this, the cylinders were rinsed five more times with de-ionised water and let drying in a fume hood. They were finally placed in a muffle furnace and baked at 500°C for 5 hours. Prior deployment they were individually sealed in teflon bags. In general, glass surfaces exhibit a low adsorption of mercury[38]. Nickel metal was chosen on the same principles based on the low degree of Hg amalgamation. On the other hand, silver metal shows a nearly quantitative collection efficiency for Hg(0) and inorganic Hg(II) species[39]. The feasibility of using silver mesh filters as passive samplers of leaching Hg was tested prior the experiment. The retention of silver mesh filter to Hg is very high (95.50% and 96.84%) and was tested by feeding a Hg standard solution at different concentrations (200 pg/ml and 500 pg/ml) through the silver mesh at a flow rate of 100 ml/h. In order to control for breakthrough, during field deployments two silver meshes were piled in each EM and analyzed separately. Negligible breakthrough was observed.

Before any field deployment, the silver meshes were blanked from Hg by positioning them in a Hg free inert gas stream and heating at 450 ^0C. This allowed reaching a stable blank value of 232.7 ± 102.6 pg (n=10). In this way the silver mesh could be reused in subsequent deployments. After repeated uses, visual inspection of the silver mesh occasionally revealed a patchwise change in the surface lustre. This might have resulted from mechanical deterioration and/or chemical oxidation. Various treatments to restore the surface were tested. Gentle treatments with diluted acid or small amount of commercial silver polish were generally found to produce a satisfactory results.

In ICP-MS measurements, isotopes of ^{198}Hg, ^{199}Hg, ^{200}Hg, ^{202}Hg of the spiked sample were collected in time-resolved, single point per-peak mode with dwell times of 20 ms. Carried gas flow was optimized every day to obtain maximum and stable signal. Detailed operating conditions for ICP-MS are listed in Table S2. A 5 ml standard solution (100 pg/ml) were measured prior to every 4-5 samples as a QA/QC measurements. Limits of detection for ICP-MS measurements of ^{202}Hg isotope was 50 pg. The forest litter spiking procedure was a critical step. For the homogeneous distribution of the spiked mercury in the organic matter, we used a diluted spiking solution via diluting 10 times the concentrated ^{202}Hg solution. In this study, 17% of the mass balance assessment of Hg in the EM provided "non-sense" negative values of Fvols. This was possibly due to poor homogeneisation of spiked litter. These outliers were excluded from statistical analysis.

Flux calculations

F_{net} (ng m^{-2} d^{-1}) is the net result of all the deposition and loss processes involving THg, and is calculated as:

$$F_{net} = \frac{\left[THg^{litter}_{native}\right]_{t_f} - \left[THg^{litter}_{native}\right]_{t_0}}{At} = F_{dep} - F_{loss} \quad (1)$$

Where $\left[THg^{litter}_{native}\right]_{t_0}$ and $\left[THg^{litter}_{native}\right]_{t_f}$ are initial and final amounts of total native Hg in the litter, respectively, A is the opening area of the EM (= 0.02 m^2) and $t=t_f-t_0$ (d) is the deployment time (here 60 d). F_{dep} represents the native Hg added through the various deposition processes to the EM during the sampling period while F_{loss} is the results of all the loss processes

F_{loss} can be further described as:

$$F_{loss} = F_{down} + F_{vol} \quad (2)$$

where, F_{down} is the downward export flux (i.e. the leaching from the EM) and F_{vol} is the volatilization flux from the organic matter. The downward transport (F^s_{down}, ng m^{-2} d^{-1}) of spiked ^{202}Hg from the litter to the silver mesh disks can be measured as follows:

$$F^s_{down} = \frac{\left[{}^{202}Hg^{silver}\right]_{t_f}}{At} \quad (3)$$

where ${}^{202}Hg^{silver}$ represent the amount of ^{202}Hg found in the silver mesh disks at the end of the exposure. Hereone the supersription "s" will indicate fluxes for ^{202}Hg. ^{202}Hg is rare in the environment, therefore the deposition flux for this isotope is approximated to be $F^s_{dep} = 0$, and equation 1 for the labeled ^{202}Hg can be rewritten as:

$$F^s_{net} = -F^s_{loss} = -\left(F^s_{down} + F^s_{vol}\right) \quad (4)$$

Let's define now the function $f_{loss_{(t)}}$ describing the instantaneous value of F_{loss}. If the concentrations of spiked ^{202}Hg in the litter is in the order of or lower than that of the native THg, and assuming the spiked ^{202}Hg behave as its native homologue, the relationship between the instantaneous loss fluxes of native and spiked ^{202}Hg can be written as:

$$f_{loss_{(t)}} = f^s_{loss_{(t)}} \quad (5)$$

where $r_{(t)} = [THg^{litter}_{native}]_t / [{}^{202}Hg^{litter}]_t$ is the ratio between the amount of native and spiked ^{202}Hg in the EM litter, and $f^s_{loss_{(t)}}$ is the istantaneous value of F^s_{loss}. Since $r_{(t)}$ is not constant (despite losses of native Hg are assumed to be the same as those of ^{202}Hg, native Hg continuously receive inputs from the atmosphere), the shape of the functions $r_{(t)}$ and $f^s_{loss_{(t)}}$ are not known. It is therefore not possible to exactly derive the value of F_{loss} for native Hg over the integrative sampling period. However, it can be argued that $r_{(t)}$ is a growing function of time, where the minimum ($r_{(t0)}$) and maximum ($r_{(tf)}$) values are experimentally known. Therefore, assuming in first approximation, that $r_{(t)}$ is linearly growing during the two month sampling period, the following relationship can be introduced as a first approximation:

$$\int_{t_0}^{t_f} r_{(t)} dt \approx \frac{\left(r_{(t_f)} + r_{(t_0)}\right)}{2} = \theta \quad (6)$$

and

$$F_{loss} = \theta F^s_{loss} \quad (7)$$

Similarly, the downward export flux and volatilization flux of native Hg from the organic matter can be expressed as:

$$F_{down} = \theta F^s_{down} \quad (8)$$

$$F_{vol} = \theta F^s_{vol} \quad (9)$$

Finally, from equation 1, 4 and 7, F_{dep} for native Hg can be calculated as follows,

$$F_{dep} = F_{net} - \theta F^s_{net} \quad (10)$$

Quality of Hg flux measurements

Screening EM flux results for measurement quality included checking for consistentcy of the following assumptions: i) the concentration of $^{202}Hg^{litter}$ is in the order or lower than that of native Hg; ii) r(t) is a growing function of time and therefore the condition assumed in equation 6 is verified; and iii) $^{202}Hg^{litter}$ is a useful tracer of the behavior of THg. Assumption i) is verified since r values representing the ratio of concentrations between THg and $^{202}Hg^{litter}$ ranged 18-20 at t(0) and 20-60 at t(f). This result also confirms the validity of assumption ii) given that $r_{(t_f)}$ was always > than $r_{(t_0)}$ (it has to be acknowledged however that the magnitude of the difference $\Delta r = r_{(t_f)} - r_{(t_0)}$, have implication for tracking the accuracy of flux measurements as described above). If the growth trend of the function r(t) is highly non linear the identity assumed in equation 6 can introduce an error. Assuming an unlikely worst case scenario with all deposition of Hg occurring only during the first day of exposure and considering the maximum observed values of Δr, it is possible to demonstrate that the resulting theoretical error in flux accuracy will not exceed 50% of the estimated mean value. Finally, assumption iii) has been adopted in other notable studies[40, 41].

It can be critically argued that the spiked ^{202}Hg could be more loosely bound to OM compared to the native Hg. A quick initial release of ^{202}Hg was indeed observed during the equilibration phase preceding the experiment, suggesting rapid volatilization of the superficially adsorbed pool. During the experiment, however, Δr values were directly correlated with the change in THg concentration in the litter at t(0) and t(f), showing that the increase in the r values are fully explained by fresh deposition of native Hg on the litter and not by higher mobilization of ^{202}Hg. An additional confirmation of is that during the sampling period of Aug-Oct and Feb-Apr, when very low net deposition of fresh THg occurred, no significant change in r values was observed.

Statistics

Normality in the distribution of replicated Hg flux measurement and litter dry mass loss was assessed using the Lillefors test with N=10. To compare Hg fluxes between canopy and gap conditions, we de-trended the dataset by dividing by dividing the individual Flux measurement for their overall (understory and clearing) mean value within each period. We obtained two groups of data (understory and clearing) and we perform a F precision test to assess similarity in their variance. We applied the Student's t-test to compare the mean of the groups in the case F-test was positive and the Cochran's variant of the t-test when variance was significantly different. Regression models were based on the ordinary least squares method. Correlation was quantified using Pearson's correlation coefficient. Significance of regression coefficients was tested by analysis of variance (ANOVA).

Organic matter analysis

Information on the method to analyze organic matter characteristics including dray weight, total OC and total N is presented in the supplementary information (Text S1).

Results and Discussion

Seasonality of litter turnover

Dry mass OC mass losses from vegetation litter measured using the EM confirmed that understory conditions significantly ($P<0.05$) promoted turnover of OM with dry mass losses up to 55% during the warmest and most humid periods (Figure 3). Dry mass loss data from the EM were validated by consistent measurements simultaneously performed using traditional litter bags in the understory. The data on litter degradation (i.e. mass loss) reveal the highly seasonal dynamic of OC respiration in this subtropical forest. The loss rate of litter mass had a maximum during the hot and wet seasons, in particular in June-August, then it consistently declined to a minimum in the dry and cold seasons, in particular January-March, to increase again with temperature and precipitation toward the last sampling campaign. During the dry and cold seasons, the litter deployed in the understory and the clearing experienced similar dry mass losses in the range of 15-25%, however the variability over time of dry and OC mass loss under the canopy was 140% of that observed in the clearing. Litter degradation rate positively correlated ($P<0.01$) with rainfall, air temperature and humidity (Table S1) both in clearing and understory.

Litter mass loss derives from the activity of detritivorous macro-invertebrates and microbe, and the loss rate depends on climate (in particular temperature and litter water content) and on the nature of the litter[42-45]. A significant decline of the C:N ratio was observed during the hot and wet seasons, consistent with the period in which the highest water content in litter was measured (Table S3). The hypothesis addressed in this study is that OC mineralization and the decline of C:N drives and correlates to Hg losses from the forest litter. Water content of litter deployed in the hot and wet seasons was generally higher than in dry and cold seasons, probably due to heavy rainfall in the hot and wet seasons. Organic matter turnover was higher in the hot and wet seasons than in the dry and cold seasons ($p<0.05$), and under the canopy compared clearing ($p<0.05$).

Experimental observations were designed to represent two blocks (understory and clearing) where environmental conditions (namely: rainfall, air temperature and humidity) were the same but distinct dynamics of OM degradation occurred. The correlation among environmental conditions data and litter dry mass, OC and N loss (Table S1) showed that OM turnover was under similar drivers both in understory and clearing conditions. The clearing conditions, however inhibited the rate of degradation, possibly due to altered water balance in the EM (e.g. more rapid evaporation in response to direct exposure to incident shortwave radiation in the clearing, compared to the understory conditions), as exhaustively discussed elsewhere[42-45, 50]. Our results on litter mass dynamics are therefore fully consistent with previous observations in similar environments[21].

Seasonality of ^{202}Hg fluxes

The F^s_{vol} and F^s_{down} fluxes in each sampling period and canopy conditions were higher in the hot and wet season than in the dry and cold season (Figure S2), suggesting that high precipitation, high temperature and enhanced dynamics of organic matter turnover favored ^{202}Hg mobilization. To our knowledge this is the first study to show a relationship between Hg mobilization from litter and OM turnover in field conditions[54, 55].

Organic matter in forest litter is largely constituted by complex polysaccharides including cellulose, more labile hemicellulose and pectine[56]. Lignin is also an important component of litter, however, unlike cellulose and hemicellulose only a limited classes of fungi and bacteria can completely mineralize it[57, 58]. The observed dependence of ^{202}Hg mobilization on litter decomposition (and the conditions that promoted it) suggests that Hg might be prevalently bound to the labile constituents. Litter mass loss derive from complete mineralization of the labile constituents and the production of water-soluble components which are

then released by leaching to the underlying soil. The leaching of water-soluble constituents may contribute to the higher values of F^{S}_{down}. Similar to soil, litter (as an organic matrix) can effectively trap Hg depositions. Litter mineralization is however fast in subtropical wet forests and tightly controlled by temperature and humidity. Previous experiments in the laboratory showed that 5%-23% Hg could be released into the atmosphere during one-year litter decomposition process due to the rapid mineralization of litter carbon[18]. In our study, higher air temperature and litter moisture during the hot and wet season, promoted faster decomposition of litter and Hg release. During the dry and cold season, instead, lower air temperature and lower litter moisture inhibited litter decomposition and Hg releases. Loss fluxes under the canopy were relatively high compared to the clearing. To this regard, it is important to recall that water budget in litter is strongly influenced by land cover. Canopies, prevent rapid evaporation of water in the litter, maintaining better conditions for microorganisms growth. Decomposition of litter has been observed to be generally faster in understories than in clearing[59-61].

The fluxes of native Hg in litter

Hg fate in litter underwent a strong climate control during the different seasons (Figure 4). The net air-litter exchange F_{net} had a positive value during October-February and April-August, and the deposition flux F_{dep} displayed a higher value in the same sampling period compared to other periods, indicating prevailing deposition of atmospheric Hg, and forest litter serving as a net sink (Figure 4). In contrast, during the other sampling periods, the loss of Hg from litter was prevalent, primarily due to re-volatilization of Hg. Generally, over the whole sampling period, both F_{vol} and F_{down} of native Hg were higher under the canopy than in the clearing. The process controlling the bulk loss of total Hg from the litter was volatilization typically representing 76% to 96% of the total loss. After de-trending to exclude the effect of seasonality, F_{loss} measured under canopy throughout the year were generally higher than in the clearing (Mann-Withney test, $P<0.05$; Figure 4). Data from the wetter and warmer part of the year were determinant for this result.

The total Hg loss from litter (F_{loss}, encompassing both volatilization and the leaching flux captured by the silver mesh) under the canopy was statistically correlated to litter dry mass loss, OC loss, N loss, rainfall, air temperature and humidity (Figure 5, Table S1). These relationships dramatically fell when considering the clearing dataset. The mean value of F_{loss} over the year ranged 520-1370 ng m^{-2} d^{-1} and 165-942 ng m^{-2} d^{-1} in the understory and clearing, respectively. These fluxes resulted in a total loss ranging between 8% and 45% in two months-time of the total Hg present in the litter at the beginning of each exposure period. The EM method allowed resolving net air/litter exchange into the volatilization and deposition component. On a yearly base, deposition of airborne Hg during litter exposure exceeded the total losses by a factor of 2.5 in the clearing and 1.5 in the understory. Vegetation litter represented therefore a net sink of atmospheric Hg. This is in agreement with previous results showing the mass of Hg in litter of temperate forests increasing over time during litter decomposition [18, 46, 47, 62]. In our study, however we observed that the general trend was inverted during certain period of the year, with volatilization higher than deposition. The mechanism of Hg accumulation during litter decomposition is still uncertain. One hypothesis is that despite ongoing decomposition, binding sites for Hg on litter OM never become saturated. In this case, accumulation mechanisms will be similar to the adsorption of Hg by the cuticle of the leaf surface[63]. Another hypothesis is that the organic functional groups formed in the litter decomposition process can also serve as new binding sites [48, 64, 65].

The first block of the experiment (understory) showed consistent results with previous laboratory-based studies in which Hg mobilization correlated with OM turnover[16-18] as well as other measured environmental variables (namely: rainfall, air temperature and humidity). The results of the second block (clearing) however, helped to disentangle the role of litter degradation as a driver of Hg loss from other correlated factors (namely: Temperature and humidity). Despite the clearing and the understory set experienced the same average conditions of temperature, waterfall and air humidity, no significant correlation was observed in the clearing with temperature and humidity. Only a positive correlation with N loss ($P<0.05$) was observed, corroborating the hypothesis that higher Hg mobilization fluxes under and outside canopies were primarily driven by litter OM turnover.

Lack of significant correlation between F_{loss} and litter dry mass loss observed in the clearing could have been determined by either lack of statistical resolution due to the limited variance of OM degradation rate (in comparison to the forest block), or by the influence of an emerging confounding factor associated to the clearing conditions, possibly controlling Hg dynamics (e.g. direct exposure to solar radiation during some hours of the day); alone or in combination. The comparison of the residuals from the correlation between F_{loss} values and the first order least square model linking F_{loss} and dry mass loss in the understory and clearing conditions helps to evaluate these cases. Consistent scedasticity (Figure S3) was observed for the residuals from the understory and clearing datasets, suggesting common drivers in the relationships linking Hg and dry mass losses. Such a consistent behaviour supports the hypothesis that: F_{loss} is under the same biogeochemical drivers in the understory and the clearing, while the lack of correlation with the OM loss flux in the clearing was likely due to the insufficient variability of OM degradation rates measured in the clearing during the year.

Total Hg loss rates observed in the present study were much higher (about one order of magnitude) than those previously observed in the laboratory-based studies[16-18] or in previous field studies[19] reporting limited mobility of OM-bounded Hg. Our study is the first to be performed in a subtropical warm and humid environment. OM degradation rates measured here were one order of magnitude higher than those reported in those previous studies[18]. Additionally, litter decomposition rate is strongly influenced by the type of litter. In general, litter decomposition rate is higher for subtropical forest dominated by evergreen or deciduous broadleaf species than for coniferous forests with pine needles[46, 66-68]. Inclusively, lower capacity of accumulating Hg in the former than the latter were also observed[47, 69]. Remarkably, the only available theoretical assessment of the influence of OM turnover on the global mass balance of Hg was performed taking into consideration parameters derived for temperate and boreal environments[9]. Subtropical and tropical forests represent more than 50% of the total forest land cover. Assessments of global mass balance of Hg could therefore have significantly underestimated the influence of rapid turnover of Hg fixed in the litter and superficial soil of subtropical and tropical humid climates. The enhanced mobility of Hg shown here deserve therefore further scientific attention, especially when assessing general fate and distribution of Hg under a globally warming climate.

Significance of EM based measurements and comparisons with previous studies

The conventional widely used technique for measuring the air-surface exchange flux of Hg(0) is the DFC method[70-72]. Hg(0) emission fluxes from deciduous forest soils previously collected using this method are summarized in Table S4. The mean volatilization flux (668 ng m^{-2} d^{-1}) calculated in the present study was somehow higher but in the sme order of magnitude than previously reported observations by DFC (Table S4) (12-498 ng m^{-2} d^{-1}) with a mean of 221 ng

m^{-2} d^{-1}. Similarly, the volatilization fluxes estimated in the present study were comparable to, although slightly higher than those measured by DFC in a study in Mt. Jinyun of Chinawhich in a similar forest ecosystem (342-498 ng m^{-2} d^{-1}) [78]. These differences are not surprising as the DFC measurements target the volatilization flux at the net of gaseous depositions, while the flux calculated through the EM represents the total volatilization. This fully explains the off-set existing between the datasets. It must also be recalled that, similarly to the EM method, DFC flux measurements are also affected by uncertainties[73-77].

Previous DFC-based measurements have shown both prevailing volatilization or depositions varying from case to case [73, 79, 80]. In contrast, measurements using the EM quantifies the total deposition flux including contributions from gaseous oxidized mercury and particulate bound mercury (PBM) dry and wet deposition (mostly from throughfall) besides the total gaseous depositions of Hg0) . Net deposition fluxes estimated from EM approach (annual mean of 276 µg m^{-2} yr^{-1}) suggested that DNNR forest was a net sink of Hg. This conclusion is also supported by earlier findings which showed that throughfall Hg fluxes (40-113 µg m^{-2} yr^{-1}) were significantly higher than the Hg(0) emission fluxes in China[79, 81-83].

Uncertainties in conventional flux measurements, and emission estimates s, (including primary and secondary sources) hinder confidence on current global and regional Hg budgets[4, 80, 84]. The proposed EM methods can constrain some of this uncertainties, delivering long term temporally integrated flux measurements. Globally, the variability of air-surface exchange flux measurements is larger for forest systems (-727 to +707 Mg yr^{-1}) than other terrestrial ecosystems[85]. Applying, in first approximation, the result generated in the present study to the total forested area of China (http://www.resdc.cn/data.aspx?DATAID=99), the net Hg deposition flux is calculate to be roughly 73 Mg yr^{-1} for the broadleaf forests and 240 Mg yr^{-1} for the coniferous forests. It should be emphasized that the air-surface exchange process strongly depends on land cover and climate[48, 49, 86, 87]. For example, THg mass positively correlated with latitude with average mass increase of 10.6 g ha^{-1} per degree latitude[48, 49]. High contents of Hg in litterfall and throughfall were observed in coniferous forests[47, 66, 88, 89], confirming boreal forests as important capacitors for Hg. It is thus recommended to expand the application of EM to address ecosystem exchange of Hg in different forest biomes.

Supporting information:

Additional information on the pearson correlation coefficients and *P* values of the correlation analysis, detailed operating conditions for ICP-MS, the trends of mean air temperature, rainfall, water content and C/N in every sampling period, Hg(0) emission fluxes from deciduous forest soils collected by DFC method, the field deployment and mass balance of Hg in the exchange meters (EMs), The fluxes of ^{202}Hg in the litter after 2 months of deployment and the consistent scedasticity for the residuals from the understory and clearing datasets.

Author information

Corresponding authors

*Tel:+86 851 85891356; Fax: +86 851 85891609; Email: fengxinbin@vip.skleg.cn

*Tel:+86 851 85891508; Fax: +86 851 85891609; Email: fuxuewu@mail.gyig.ac.cn

*Tel:+47 22 18 51 00; Fax: +47 22 18 52 00; Email: luca.nizzetto@niva.no

Acknowledgments

This research was financially supported by Research Council of Norway under the programme NORKLIMA “Mechanisms of the air-surface exchange of organic pollutants and mercury in a Chinese subtropical forest (EXPOLL, 193608/S30 2010-2012)” and also supported by the National Science Foundation of China (41430754, 41703134, 41622305). We also thank Xiang Liu, Lili Ming, Liwei Cui, and Yupeng Cheng for their assistance with sampling and analysis.

References

1. Lindberg, S. E.; Stratton, W. J., Atmospheric mercury speciation: Concentrations and behavior of reactive gaseous mercury in ambient air. *Environ Sci Technol* 1998, *32*, (1), 49-57.

2. St Louis, V. L.; Rudd, J. W. M.; Kelly, C. A.; Hall, B. D.; Rolfhus, K. R.; Scott, K. J.; Lindberg, S. E.; Dong, W., Importance of the forest canopy to fluxes of methyl mercury and total mercury to boreal ecosystems. *Environ Sci Technol* 2001, *35*, (15), 3089-3098.

3. Poissant, L.; Pilote, M.; Xu, X. H.; Zhang, H.; Beauvais, C., Atmospheric mercury speciation and deposition in the Bay St. Francois wetlands. *J Geophys Res-Atmos* 2004, *109*, (D11), doi:10.1029/2003JD004364.

4. Pirrone, N.; Cinnirella, S.; Feng, X.; Finkelman, R. B.; Friedli, H. R.; Leaner, J.; Mason, R.; Mukherjee, A. B.; Stracher, G. B.; Streets, D. G.; Telmer, K., Global mercury emissions to the atmosphere from anthropogenic and natural sources. *Atmos Chem Phys* 2010, *10*, (13), 5951-5964.

5. Gustin, M. S.; Engle, M.; Ericksen, J.; Xin, M.; Krabbenhoft, D.; Lindberg, S.; Olund, S.; Rytuba, J., New insights into mercury exchange between air and substrate. *Geochim Cosmochim Ac* 2005, *69*, (10), A700-A700.

6. Laacouri, A.; Nater, E. A.; Kolka, R. K., Distribution and Uptake Dynamics of Mercury in Leaves of Common Deciduous Tree Species in Minnesota, USA. *Environ Sci Technol* 2013, *47*, (18), 10462-10470.

7. Wang, X.; Bao, Z. D.; Lin, C. J.; Yuan, W.; Feng, X. B., Assessment of Global Mercury Deposition through Litterfall. *Environ Sci Technol* 2016, *50*, (16), 8548-8557.

8. Jiskra, M.; Sonke, J. E.; Obrist, D.; Bieser, J.; Ebinghaus, R.; Myhre, C. L.; Pfaffhuber, K. A.; Wangberg, I.; Kyllonen, K.; Worthy, D.; Martin, L. G.; Labuschagne, C.; Mkololo, T.; Ramonet, M.; Magand, O.; Dommergue, A., A vegetation control on seasonal variations in global atmospheric mercury concentrations. *Nat Geosci* 2018, *11*, (4), 244-250.

9. Smith-Downey, N. V.; Sunderland, E. M.; Jacob, D. J., Anthropogenic impacts on global storage and emissions of mercury from terrestrial soils: Insights from a new global model. *Journal of Geophysical Research-Biogeosciences* 2010, 115, doi:10.1029/2009JG001124.
10. Farella, N.; Lucotte, M.; Davidson, R.; Daigle, S., Mercury release from deforested soils triggered by base cation enrichment. *Science of the Total Environment* 2006, *368*, (1), 19-29.
11. Manceau, A.; Wang, J. X.; Rovezzi, M.; Glatzel, P.; Feng, X. B., Biogenesis of Mercury-Sulfur Nanoparticles in Plant Leaves from Atmospheric Gaseous Mercury. *Environ Sci Technol* 2018, *52*, (7), 3935-3948.
12. Tsui, M. T. K.; Finlay, J. C.; Nater, E. A., Effects of Stream Water Chemistry and Tree Species on Release and Methylation of Mercury during Litter Decomposition. *Environ Sci Technol* 2008, *42*, (23), 8692-8697.
13. Zhang, H.; Lindberg, S. E., Processes influencing the emission of mercury from soils: A conceptual model. *J Geophys Res-Atmos* 1999, *104*, (D17), 21889-21896.
14. Skyllberg, U.; Xia, K.; Bloom, P. R.; Nater, E. A.; Bleam, W. F., Binding of mercury(II) to reduced sulfur in soil organic matter along upland-peat soil transects. *Journal of Environmental Quality* 2000, *29*, (3), 855-865.
15. Khwaja, A. R.; Bloom, P. R.; Brezonik, P. L., Binding constants of divalent mercury (Hg2+) in soil humic acids and soil organic matter. *Environmental Science & Technology* 2006, *40*, (3), 844-849.
16. Fritsche, J.; Obrist, D.; Alewell, C., Evidence of microbial control of Hg-0 emissions from uncontaminated terrestrial soils. *Journal of Plant Nutrition and Soil Science-Zeitschrift Fur Pflanzenernahrung Und Bodenkunde* 2008, *171*, (2), 200-209.
17. Obrist, D.; FaÃ¯n, X.; Berger, C., Gaseous elemental mercury emissions and CO2 respiration rates in terrestrial soils under controlled aerobic and anaerobic laboratory conditions. *Science of The Total Environment* 2010, *408*, (7), 1691-1700.
18. Pokharel, A. K.; Obrist, D., Fate of mercury in tree litter during decomposition. *Biogeosciences* 2011, *8*, (9), 2507-2521.
19. Hintelmann, H.; Harris, R.; Heyes, A.; Hurley, J. P.; Kelly, C. A.; Krabbenhoft, D. P.; Steve Lindberg, O.; Rudd, J. W. M.; Scott, K. J.; Louis, V. L. S., Reactivity and mobility of new and old mercury deposition in a boreal forest ecosystem during the first year of the METAALICUS study. *ENVIRONMENTAL SCIENCE & TECHNOLOGY* 2002, *36*, (23), 5034-5040.
20. Wang, X.; Lin, C. J.; Lu, Z. Y.; Zhang, H.; Zhang, Y. P.; Feng, X. B., Enhanced accumulation and storage of mercury on subtropical evergreen forest floor: Implications on mercury budget in global forest ecosystems. *J Geophys Res-Biogeo* 2016, *121*, (8), 2096-2109.
21. Zhang, Q. H.; Zak, J. C., Effects of Gap Size on Litter Decomposition and Microbial Activity in a Subtropical Forest. *Ecology* 1995, *76*, (7), 2196-2204.
22. Zhang N a, Q. Y. u.-n., Liu X i ng -zhao,Chu Guo -we i, Zhang De -qiang, YanJun -hua, Nutrient Characteristics in Incident Rai nfall , Throughfall , and stemflow in Monsoon Evergreen Broad -leaved Forest at Dinghushan. *Journal of Tropical and Subtropical Botany* 2010, *18*, (5), 502~ 510.
23. Zhiyong, L. X. W. X. Z. S. W. Y. D. H. H. Z. C. Y. B. R. W., VARIATION AND SOURCE ANALYSIS OF ATMOSPHERIC ORGANIC ACIDS FROM PRECIPITATION AT DINGHU MOUNTAIN. *ENVIRONMENTAL CHEMISTRY* 2011, *30*, (9), 1612-1619.
24. Wang Chunlin, Z. G., Wang Xu1; , T. X., Zhou Chuanyan, Yu Guirui; , Below-canopy CO2 flux and its environmental response characteristics in a coniferous and broad-leaved mixed forest in Dinghushan, China. *Acta Ecologica Sinica* 2007, *27*, (3), 846-854.
25. Lindberg, S. E.; Meyers, T. P.; Taylor, G. E.; Turner, R. R.; Schroeder, W. H., Atmosphere-Surface Exchange of Mercury in a Forest - Results of Modeling and Gradient Approaches. *J Geophys Res-Atmos* 1992, *97*, (D2), 2519-2528.
26. Frescholtz, T. F.; Gustin, M. S.; Schorran, D. E.; Fernandez, G. C. J., Assessing the source of mercury in foliar tissue of quaking aspen. *Environ Toxicol Chem* 2003, *22*, (9), 2114-2119.
27. Sheehan, K. D.; Fernandez, I. J.; Kahl, J. S.; Amirbahman, A., Litterfall mercury in two forested watersheds at Acadia National Park, Maine, USA. *Water Air Soil Poll* 2006, *170*, (1-4), 249-265.
28. Carrasco-Gil, S.; Siebner, H.; LeDuc, D. L.; Webb, S. M.; Millan, R.; Andrews, J. C.; Hernandez, L. E., Mercury Localization and Speciation in Plants Grown Hydroponically or in a Natural Environment. *Environ Sci Technol* 2013, *47*, (7), 3082-3090.
29. Jiskra, M.; Wiederhold, J. G.; Skyllberg, U.; Kronberg, R. M.; Hajdas, I.; Kretzschmar, R., Mercury Deposition and Re-emission Pathways in Boreal Forest Soils Investigated with Hg Isotope Signatures. *Environ Sci Technol* 2015, *49*, (12), 7188-7196.
30. Zhou, J.; Feng, X. B.; Liu, H. Y.; Zhang, H.; Fu, X. W.; Bao, Z. D.; Wang, X.; Zhang, Y. P., Examination of total mercury inputs by precipitation and litterfall in a remote upland forest of Southwestern China. *Atmos Environ* 2013, *81*, 364-372.
31. Wang, J.; Feng, X.; Anderson, C. W. N.; Qiu, G.; Ping, L.; Bao, Z., Ammonium thiosulphate enhanced phytoextraction from mercury contaminated soil–Results from a greenhouse study. *Journal of hazardous materials* 2011, *186*, (1), 119-127.
32. Olson, M. L.; DeWild, J. F. In *Techniques for the collection and species-specific analysis of low levels of mercury in water, sediment, and biota*, 1999; 1999; pp 191-201.
33. Feng, X.; Li, P.; Qiu, G.; Wang, S.; Li, G.; Shang, L.; Meng, B.; Jiang, H.; Bai, W.; Li, Z., Human exposure to methylmercury through rice intake in mercury mining areas, Guizhou Province, China. *ENVIRONMENTAL SCIENCE & TECHNOLOGY* 2007, *42*, (1), 326-332.
34. Hintelmann, H.; Ogrinc, N., Determination of stable mercury isotopes by ICP/MS and their application in environmental studies. *Acs Sym Ser* 2003, *835*, 321-338.
35. Wang, R.; Feng, X. B.; Wang, W. X., In Vivo Mercury Methylation and Demethylation in Freshwater Tilapia Quantified by Mercury Stable Isotopes. *Environ Sci Technol* 2013, *47*, (14), 7949-7957.

368 36. Cui, L. W.; Feng, X. B.; Lin, C. J.; Wang, X. M.; Meng, B.; Wang, X.; Wang, H., Accumulation and Translocation of (198)Hg in Four Crop
369 Species. *Environ Toxicol Chem* 2014, *33*, (2), 334-340.
370 37. Blum, J. D., Applications of stable mercury isotopes to biogeochemistry. *Handbook of Environmental Isotope Geochemistry* 2011, 229-245.
371 38. Spedding, D. J.; Hamilton, R. B., Adsorption of Mercury-Vapor by Indoor Surfaces. *Environ Res* 1982, *29*, (1), 30-41.
372 39. Dumarey, R.; Dams, R.; Hoste, J., Comparison of the collection and desorption efficiency of activated charcoal, silver, and gold for the
373 determination of vapor-phase atmospheric mercury. *Analytical Chemistry* 1985, *57*, (13), 2638-2643.
374 40. Hintelmann, H.; Harris, R.; Heyes, A.; Hurley, J. P.; Kelly, C. A.; Krabbenhoft, D. P.; Lindberg, S.; Rudd, J. W.; Scott, K. J.; St. Louis, V. L.,
375 Reactivity and mobility of new and old mercury deposition in a boreal forest ecosystem during the first year of the METAALICUS study. *Environmental*
376 *science & technology* 2002, *36*, (23), 5034-5040.
377 41. Ericksen, J. A.; Gustin, M. S.; Lindberg, S. E.; Olund, S. D.; Krabbenhoft, D. P., Assessing the potential for re-emission of mercury deposited in
378 precipitation from arid soils using a stable isotope. *Environmental science & technology* 2005, *39*, (20), 8001-8007.
379 42. McClaugherty, C. A.; Pastor, J.; Aber, J. D.; Melillo, J. M., Forest litter decomposition in relation to soil nitrogen dynamics and litter quality.
380 *Ecology* 1985, 266-275.
381 43. Hobbie, S. E., Temperature and plant species control over litter decomposition in Alaskan tundra. *Ecological Monographs* 1996, *66*, (4), 503-522.
382 44. Jianfen, G.; Yusheng, Y.; Guangshui, C.; Peng, L.; Jinsheng, X., A review on litter decomposition in forest ecosystem. *Scientia Silvae Sinicae*
383 2006, *42*, (4), 93-100.
384 45. O'CONNELL, A., Litter decomposition, soil respiration and soil chemical and biochemical properties at three contrasting sites in karri (Eucalyptus
385 diversicolor F. Muell.) forests of south‐western Australia. *Australian journal of ecology* 1987, *12*, (1), 31-40.
386 46. Hall, B. D.; Louis, V. L. S., Methylmercury and total mercury in plant litter decomposing in upland forests and flooded landscapes. *Environ Sci*
387 *Technol* 2004, *38*, (19), 5010-5021.
388 47. Demers, J. D.; Driscoll, C. T.; Fahey, T. J.; Yavitt, J. B., Mercury cycling in litter and soil in different forest types in the Adirondack region, New
389 York, USA. *Ecol Appl* 2007, *17*, (5), 1341-1351.
390 48. Obrist, D.; Johnson, D. W.; Lindberg, S. E.; Luo, Y.; Hararuk, O.; Bracho, R.; Battles, J. J.; Dail, D. B.; Edmonds, R. L.; Monson, R. K.; Ollinger,
391 S. V.; Pallardy, S. G.; Pregitzer, K. S.; Todd, D. E., Mercury Distribution Across 14 US Forests. Part I: Spatial Patterns of Concentrations in Biomass,
392 Litter, and Soils. *Environ Sci Technol* 2011, *45*, (9), 3974-3981.
393 49. Obrist, D., Mercury Distribution across 14 U.S. Forests. Part II: Patterns of Methyl Mercury Concentrations and Areal Mass of Total and Methyl
394 Mercury. *Environ Sci Technol* 2012, *46*, (11), 5921-5930.
395 50. Swift, M., Heal, 0. W. & Anderson, JM (1979). Decomposition in Terrestrial Ecosystems. *Studies in ecology 5*.
396 51. Lindberg, S. E.; Harriss, R. C., Mercury-Organic Matter Associations in Estuarine Sediments and Interstitial Water. *Environ Sci Technol* 1974, *8*,
397 (5), 459-462.
398 52. Kolka, R. K.; Grigal, D. F.; Verry, E. S.; Nater, E. A., Mercury and organic carbon relationships in streams draining forested upland peatland
399 watersheds. *J Environ Qual* 1999, *28*, (3), 766-775.
400 53. Kolka, R. K.; Nater, E. A.; Grigal, D. F.; Verry, E. S., Atmospheric inputs of mercury and organic carbon into a forested upland bog watershed.
401 *Water Air Soil Poll* 1999, *113*, (1-4), 273-294.
402 54. Hissler, C.; Probst, J. L., Impact of mercury atmospheric deposition on soils and streams in a mountainous catchment (Vosges, France) polluted
403 by chlor-alkali industrial activity: The important trapping role of the organic matter. *SCIENCE OF THE TOTAL ENVIRONMENT* 2006, *361*, (1), 163-
404 178.
405 55. Laurier, F.; Cossa, D.; Gonzalez, J. L.; Breviere, E.; Sarazin, G., Mercury transformations and exchanges in a high turbidity estuary::: The role of
406 organic matter and amorphous oxyhydroxides. *Geochimica et cosmochimica acta* 2003, *67*, (18), 3329-3345.
407 56. Kogel-Knabner, I., The macromolecular organic composition of plant and microbial residues as inputs to soil organic matter. *Soil Biol Biochem*
408 2002, *34*, (2), 139-162.
409 57. Bugg, T. D. H.; Ahmad, M.; Hardiman, E. M.; Rahmanpour, R., Pathways for degradation of lignin in bacteria and fungi. *Nat Prod Rep* 2011, *28*,
410 (12), 1883-1896.
411 58. Longe, L. F.; Couvreur, J.; Grandchamp, M. L.; Garnier, G.; Allais, F.; Saito, K., Importance of Mediators for Lignin Degradation by Fungal
412 Laccase. *Acs Sustain Chem Eng* 2018, *6*, (8), 10097-10107.
413 59. Ferreira, V.; Chauvet, E., Future increase in temperature more than decrease in litter quality can affect microbial litter decomposition in streams.
414 *Oecologia* 2011, *167*, (1), 279-291.
415 60. Yin, X. W.; Perry, J. A.; Dixon, R. K., Influence of Canopy Removal on Oak Forest Floor Decomposition. *Can J Forest Res* 1989, *19*, (2), 204-
416 214.
417 61. Whitford, W. G.; Meentemeyer, V.; Seastedt, T. R.; Cromack, K.; Crossley, D. A.; Santos, P.; Todd, R. L.; Waide, J. B., Exceptions to the Aet
418 Model - Deserts and Clear-Cut Forest. *Ecology* 1981, *62*, (1), 275-277.
419 62. Ma, M.; Du, H. X.; Wang, D. Y.; Sun, T.; Sun, S. W.; Yang, G., The fate of mercury and its relationship with carbon, nitrogen and bacterial
420 communities during litter decomposing in two subtropical forests. *Appl Geochem* 2017, *86*, 26-35.
421 63. Stamenkovic, J.; Gustin, M. S., Nonstomatal versus Stomatal Uptake of Atmospheric Mercury. *Environ Sci Technol* 2009, *43*, (5), 1367-1372.

64. Demers, J. D.; Yavitt, J. B.; Driscoll, C. T.; Montesdeoca, M. R., Legacy mercury and stoichiometry with C, N, and S in soil, pore water, and stream water across the upland-wetland interface: The influence of hydrogeologic setting. *J Geophys Res-Biogeo* 2013, *118*, (2), 825-841.
65. Navratil, T.; Shanley, J.; Rohovec, J.; Hojdova, M.; Penizek, V.; Buchtova, J., Distribution and Pools of Mercury in Czech Forest Soils. *Water Air Soil Poll* 2014, *225*, (3), doi:10.1007/s11270-013-1829-1.
66. Gruba, P.; Socha, J.; Pietrzykowski, M.; Pasichnyk, D., Tree species affects the concentration of total mercury (Hg) in forest soils: Evidence from a forest soil inventory in Poland. *Sci Total Environ* 2019, *647*, 141-148.
67. Blackwell, B. D.; Driscoll, C. T., Using foliar and forest floor mercury concentrations to assess spatial patterns of mercury deposition. *Environ Pollut* 2015, *202*, 126-134.
68. Schwesig, D.; Matzner, E., Dynamics of mercury and methylmercury in forest floor and runoff of a forested watershed in Central Europe. *Biogeochemistry* 2001, *53*, (2), 181-200.
69. Zhou, J.; Wang, Z. W.; Zhang, X. S., Deposition and Fate of Mercury in Litterfall, Litter, and Soil in Coniferous and Broad-Leaved Forests. *J Geophys Res-Biogeo* 2018, *123*, (8), 2590-2603.
70. Feng, X. B.; Wang, S. F.; Qiu, G. A.; Hou, Y. M.; Tang, S. L., Total gaseous mercury emissions from soil in Guiyang, Guizhou, China. *J Geophys Res-Atmos* 2005, *110*, (D14), doi:10.1029/2004JD005643.
71. Gustin, M. S.; Rasmussen, P.; Edwards, G.; Schroeder, W.; Kemp, J., Application of a laboratory gas exchange chamber for assessment of in situ mercury emissions. *J Geophys Res-Atmos* 1999, *104*, (D17), 21873-21878.
72. Xiao, Z. F.; Munthe, J.; Schroeder, W. H.; Lindqvist, O., Vertical Fluxes of Volatile Mercury over Forest Soil and Lake Surfaces in Sweden. *Tellus B* 1991, *43*, (3), 267-279.
73. Gustin, M. S.; Lindberg, S. E., Assessing the contribution of natural sources to the global mercury cycle: The importance of intercomparing dynamic flux measurements. *Fresen J Anal Chem* 2000, *366*, (5), 417-422.
74. Eckley, C. S.; Gustin, M.; Lin, C. J.; Li, X.; Miller, M. B., The influence of dynamic chamber design and operating parameters on calculated surface-to-air mercury fluxes. *Atmos Environ* 2010, *44*, (2), 194-203.
75. Lin, C. J.; Zhu, W.; Li, X. C.; Feng, X. B.; Sommar, J.; Shang, L. H., Novel Dynamic Flux Chamber for Measuring Air-Surface Exchange of Hg-o from Soils. *Environ Sci Technol* 2012, *46*, (16), 8910-8920.
76. Zhu, W.; Sommar, J.; Lin, C. J.; Feng, X., Mercury vapor air-surface exchange measured by collocated micrometeorological and enclosure methods - Part II: Bias and uncertainty analysis. *Atmos Chem Phys* 2015, *15*, (10), 5359-5376.
77. Zhu, W.; Sommar, J.; Lin, C. J.; Feng, X., Mercury vapor air-surface exchange measured by collocated micrometeorological and enclosure methods - Part I: Data comparability and method characteristics. *Atmos Chem Phys* 2015, *15*, (2), 685-702.
78. Ma, M.; Wang, D. Y.; Sun, R. G.; Shen, Y. Y.; Huang, L. X., Gaseous mercury emissions from subtropical forested and open field soils in a national nature reserve, southwest China. *Atmos Environ* 2013, *64*, 116-123.
79. Fu, X. W.; Feng, X. B.; Sommar, J.; Wang, S. F., A review of studies on atmospheric mercury in China. *Sci Total Environ* 2012, *421*, 73-81.
80. Zhu, W.; Lin, C. J.; Wang, X.; Sommar, J.; Fu, X. W.; Feng, X. B., Global observations and modeling of atmosphere-surface exchange of elemental mercury: a critical review. *Atmos Chem Phys* 2016, *16*, (7), 4451-4480.
81. Ma, M.; Wang, D. Y.; Du, H. X.; Sun, T.; Zhao, Z.; Wang, Y. M.; Wei, S. Q., Mercury dynamics and mass balance in a subtropical forest, southwestern China. *Atmos Chem Phys* 2016, *16*, (7), 4529-4537.
82. Wang, Z. W.; Zhang, X. S.; Xiao, J. S.; Zhijia, C.; Yu, P. Z., Mercury fluxes and pools in three subtropical forested catchments, southwest China. *Environ Pollut* 2009, *157*, (3), 801-808.
83. Zhou, J.; Wang, Z. W.; Sun, T.; Zhang, H.; Zhang, X. S., Mercury in terrestrial forested systems with highly elevated mercury deposition in southwestern China: The risk to insects and potential release from wildfires. *Environ Pollut* 2016, *212*, 188-196.
84. Song, S.; Selin, N. E.; Soerensen, A. L.; Angot, H.; Artz, R.; Brooks, S.; Brunke, E. G.; Conley, G.; Dommergue, A.; Ebinghaus, R.; Holsen, T. M.; Jaffe, D. A.; Kang, S.; Kelley, P.; Luke, W. T.; Magand, O.; Marumoto, K.; Pfaffhuber, K. A.; Ren, X.; Sheu, G. R.; Slemr, F.; Warneke, T.; Weigelt, A.; Weiss-Penzias, P.; Wip, D. C.; Zhang, Q., Top-down constraints on atmospheric mercury emissions and implications for global biogeochemical cycling. *Atmos Chem Phys* 2015, *15*, (12), 7103-7125.
85. Agnan, Y.; Le Dantec, T.; Moore, C. W.; Edwards, G. C.; Obrist, D., New Constraints on Terrestrial Surface Atmosphere Fluxes of Gaseous Elemental Mercury Using a Global Database. *Environ Sci Technol* 2016, *50*, (2), 507-524.
86. de Lima, C. A. I.; de Almeida, M. G.; Pestana, I. A.; Bastos, W. R.; Recktenvald, M. C. N. D.; de Souza, C. M. M.; Pedrosa, P., Impact of Land Use on the Mobility of Hg Species in Different Compartments of a Tropical Watershed in Brazil. *Arch Environ Con Tox* 2017, *73*, (4), 578-592.
87. Zhang, L. M.; Wu, Z. Y.; Cheng, I.; Wright, L. P.; Olson, M. L.; Gay, D. A.; Risch, M. R.; Brooks, S.; Castro, M. S.; Conley, G. D.; Edgerton, E. S.; Holsen, T. M.; Luke, W.; Tordon, R.; Weiss-Penzias, P., The Estimated Six-Year Mercury Dry Deposition Across North America. *Environ Sci Technol* 2016, *50*, (23), 12864-12873.
88. Risch, M. R.; DeWild, J. F.; Gay, D. A.; Zhang, L. M.; Boyer, E. W.; Krabbenhoft, D. P., Atmospheric mercury deposition to forests in the eastern USA. *Environ Pollut* 2017, *228*, 8-18.
89. Lu, W. J.; Liu, N.; Zhang, Y. J.; Zhou, J. Q.; Guo, Y. P.; Yang, X., Impact of vegetation community on litter decomposition: Evidence from a reciprocal transplant study with C-13 labeled plant litter. *Soil Biol Biochem* 2017, *112*, 248-257.

Figure 1: The location of sampling site DNNR (Yellow circle) and gridded (0.1°×0.1°) mean of monthly NDVI (satellite-based normalized difference vegetation index, representing the vegetation activity) in East Asia during the study period.[8]

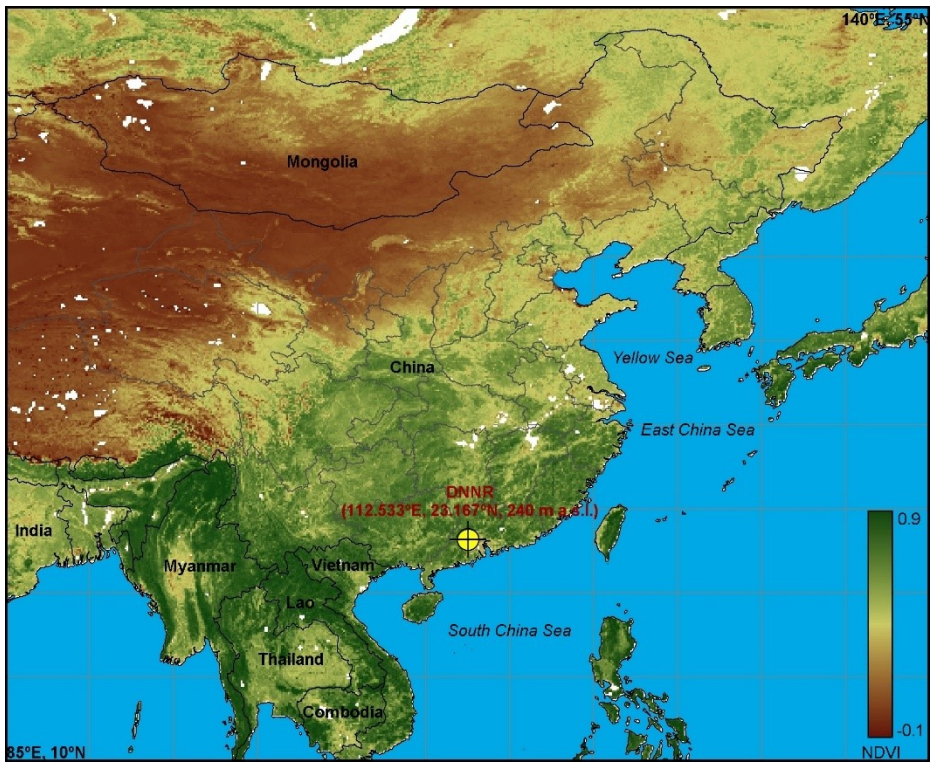

Figure 2: The diagram of the exchange meters (EMs). F_{dep} was the Hg flux deposited to the EM during the sampling period, F_{down} is the Hg flux downward export (e.g. leaching (including run-off) from EM and F_{vol} is the Hg flux emitted up to the air from EM.

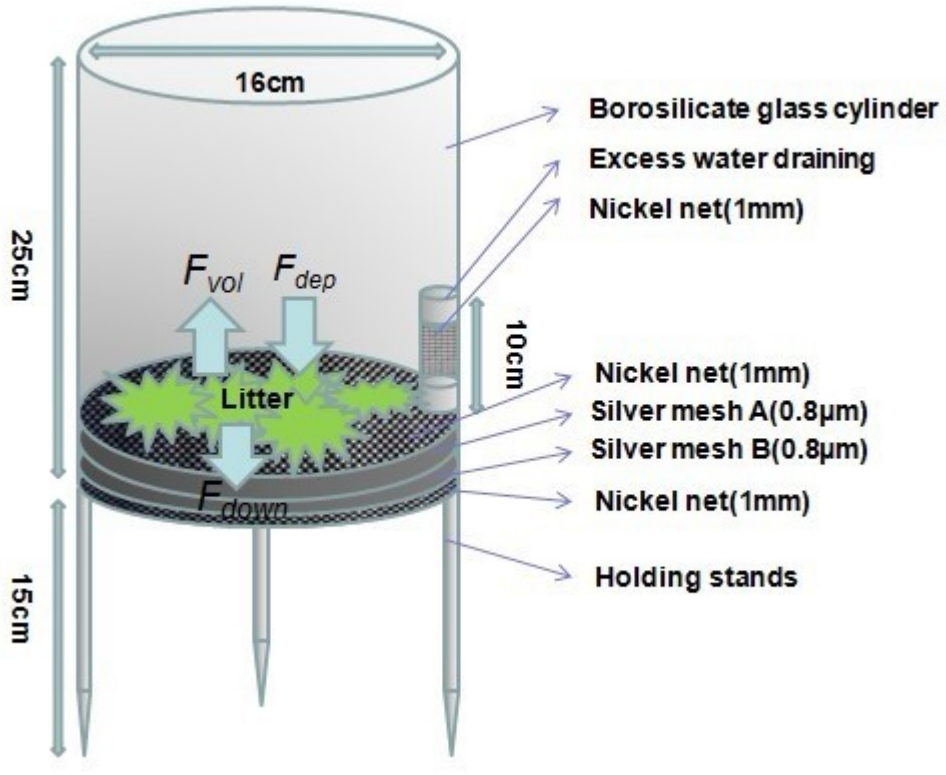

530

531

532

533

534

535

536

537

538

539

540

541

542

543

544

545

546

547

548 **Figure 3.** Bow plots of the litter dry mass loss expressed as percentage of the initial dry mass for the understory (grey boxes) and the
549 clearing. Boxes show sample mean, 25th and 75th percentiles. Whiskers extent to the lowest (or highest) value within 1.5 of the lower (or
550 higher, respectively) interquartile range.

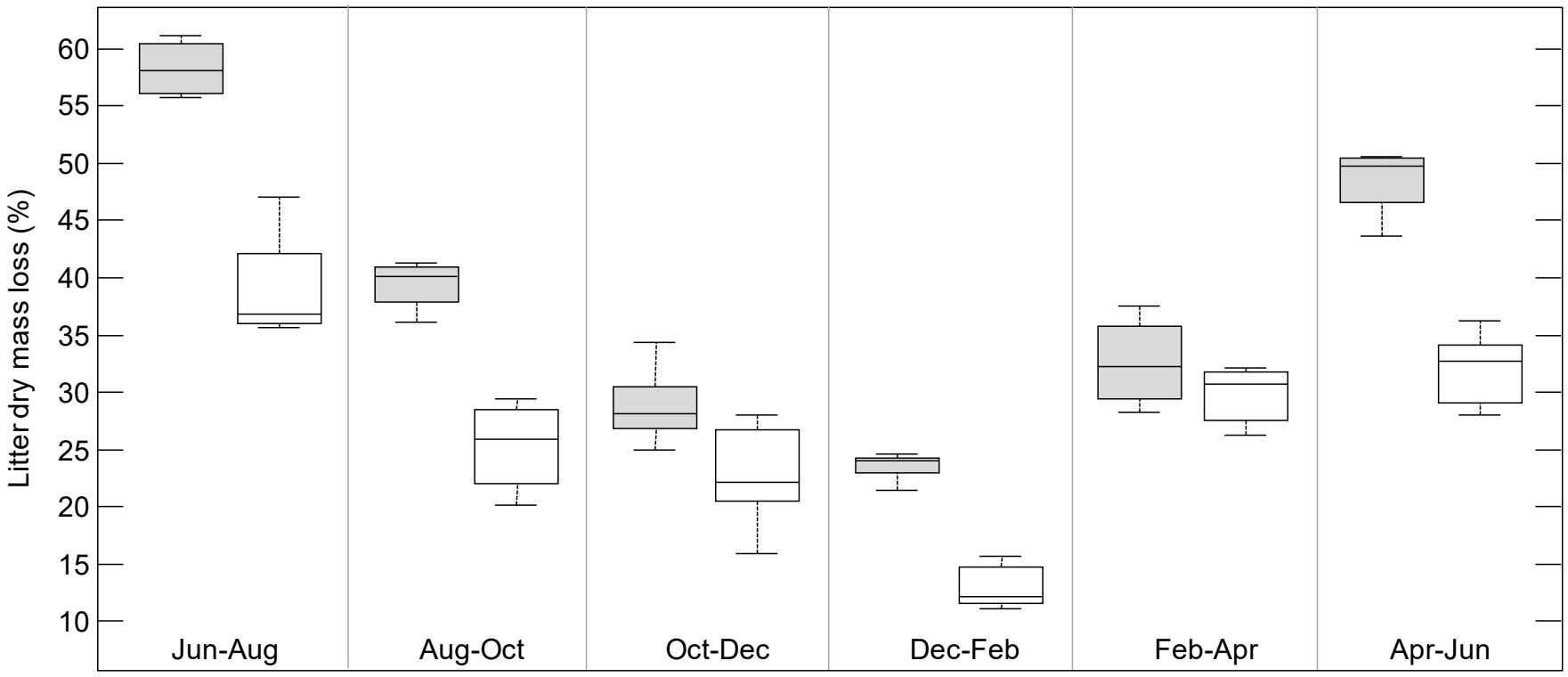

551
552
553
554
555
556
557
558
559
560
561
562
563
564
565
566
567
568
569
570

Figure 4. Hg loss, deposition and net fluxes of native Hg as well as their volatilization and leaching components in the litter after 2 months of deployment. (a) Left (black) bars represent the leaching fluxes of native Hg (F_{down}) in the understory and right (gray) bars represent the leaching fluxes of native Hg (F_{down}) in the clearing. (b) Left (dark blue) bars represent the volatilization fluxes of native Hg (F_{vol}) in the understory and right (blue) bars represent the volatilization fluxes of native Hg (F_{vol}) in the clearing. (c) Left (black) bars represent the loss fluxes of native Hg (F_{loss}) in the understory and right (red) bars represent the loss fluxes of native Hg (F_{loss}) in the clearing. (d) Left (dark green) bars represent the deposition fluxes of native Hg (F_{dep}) in the understory and right (bright green) bars represent the deposition fluxes of native Hg (F_{dep}) in the clearing. (e) Left (dark red) bars represent the net fluxes of native Hg (F_{net}) in the understory and right (light green) bars represent the net fluxes of native Hg (F_{net}) in the clearing.

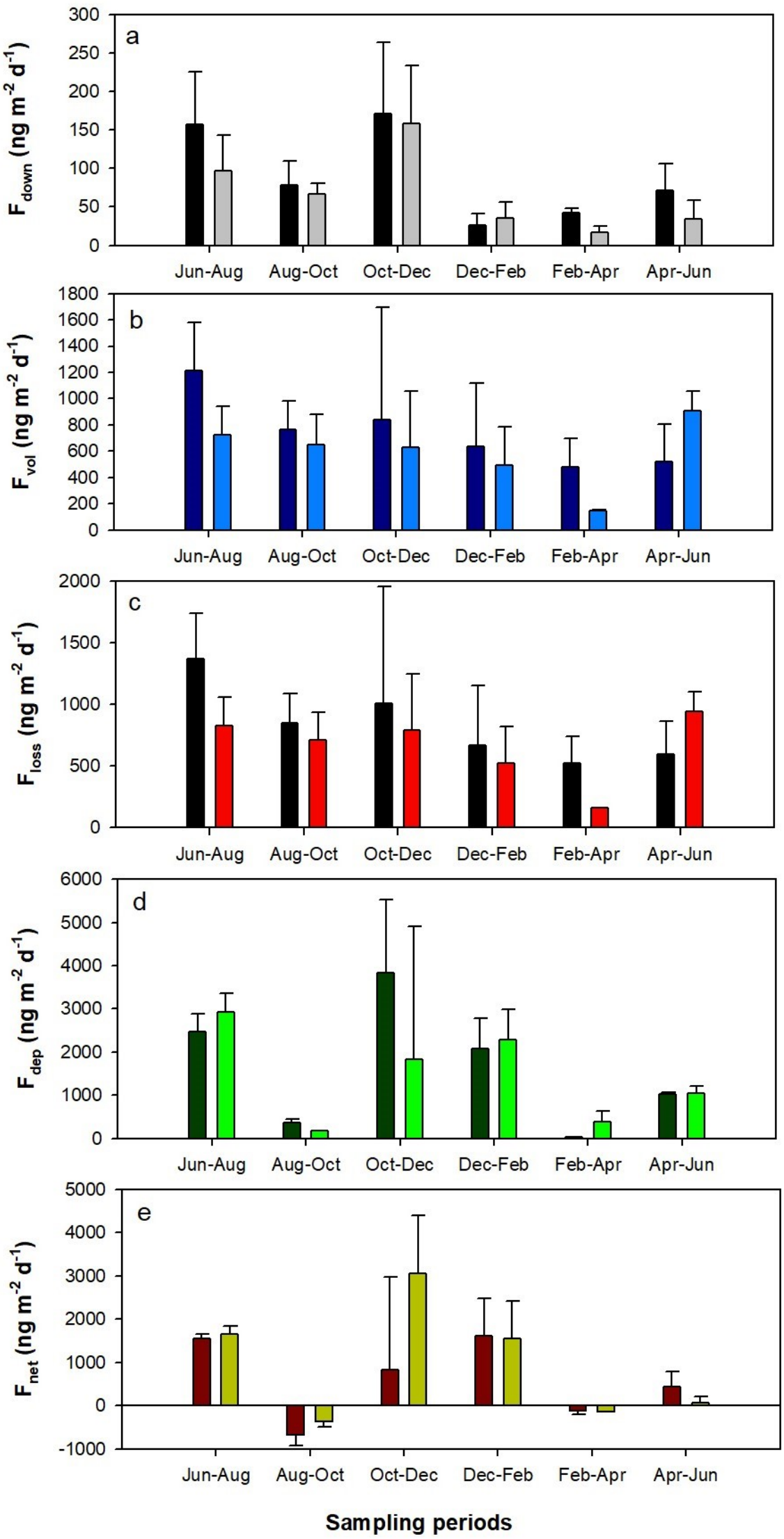

581 **Figure 5.** Scatter plot and first order least square model for F_{loss} vs litter dry mass loss.

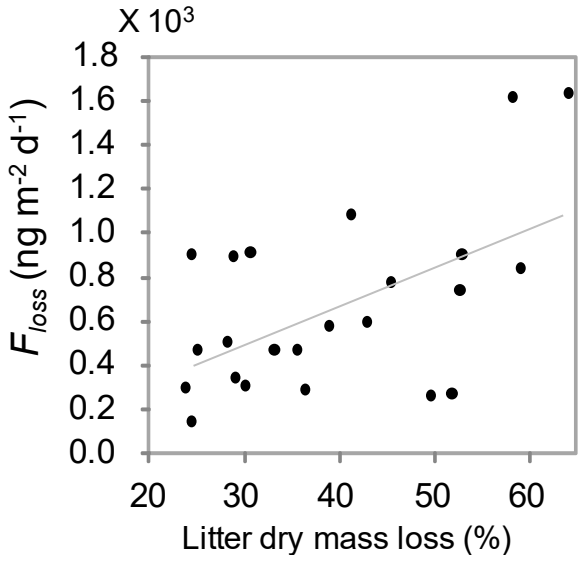

582